Electronic Supplementary Material (ESI) for Journal of Materials Chemistry A.

Supporting Information

Atmospheric pressure chemical vapor deposition of methylammonium bismuth iodide perovskites

Xiao Chen[1], Yoon Myung[1,2], Arashdeep Thind[3], Zhengning Gao[3], Bo Yin[3], Sung Beom Cho[1], Peifu Cheng[1], Bryce Sadtler[3,4], Rohan Mishra[1,3], Parag Banerjee[1,3]

[1]Department of Mechanical Engineering and Materials Science, Washington University in St. Louis, St. Louis, MO – 63130, USA

[2]Department of Nanotechnology and Advanced Materials Engineering, Sejong University, Seoul, 05006, Korea

[3]Institute of Materials Science & Engineering, Washington University in St. Louis, St. Louis, MO – 63130, USA

[4]Department of Chemistry, Washington University in St. Louis, St. Louis, MO – 63130, USA

Supporting Information S1: X-ray diffration of MAI powder

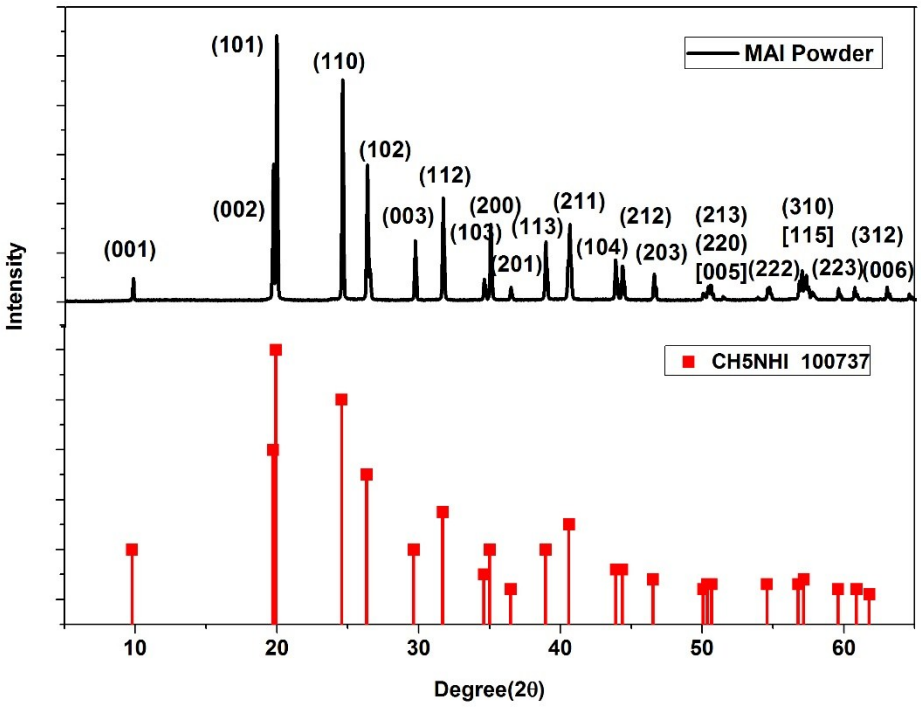

Figure S 1: XRD of MAI powder (black) with corresponding JCPDS file # 100737 in red below.

Supporting Information S2: Calculation of vapor pressure for BiI_3 and ratio of MAI and BiI_3 vapor pressures at point of sublimation and condensation

Thermogravimetric analysis (TGA) is used to determine the mass loss behavior of the methyl ammonium iodide (MAI) and bismuth iodide (BiI_3) powders. These are the constituents that make up the perovskite, $(CH_3NH_3)_3Bi_2I_9$. TGA was performed using Q5000 IR (TA Instruments), heating at a steady heating rate (typically between 2.5 and 10 °C min^{-1}) under a constant 20 mL min^{-1} N_2 gas flow. The investigated temperature intervals were between a minimum of 25 °C to a maximum of 800 °C. Ceramic crucibles and approximately 5−15 mg of sample material were employed for each measurement. The approach presented here is adapted from Dualeh et al.,[1] and the data for MAI is directly obtained from their analysis. The data for BiI_3 is obtained from our experiments, as described below.

The Clausius-Clapeyron relation relates the vapor pressure p and the temperature T of a solid with its enthalpy of sublimation ΔH_{sub}, where R is the gas constant ($8.314 JK^{-1}mol^{-1}$) according to equation S1[2]

$$\frac{d \ln p}{dt} = \frac{\Delta H_{sub}}{RT^2} \qquad \text{[eq. S1]}$$

The first derivative of the TGA heat curve gives a direct measure of the instantaneous rate of mass loss m_{sub} at temperature T,

$$\frac{dm}{dt} = \frac{\Delta m}{\Delta t} = m_{sub} \qquad \text{[eq. S2]}$$

In equilibrium conditions, the rates of vapor condensation and evaporation are assumed to be equal. Hence the rate of mass loss by sublimation m_{sub} can be related to the vapor pressure by equation S3 according to Langmuir[3] where A is the exposed sublimation surface area (here we

take the area calculated from the TGA sample pan during the measurement) and M_w is the molecular mass of the material.

$$p = \frac{1}{A}\left(\frac{2\pi RT}{M_w}\right)^{\frac{1}{2}} m_{sub} \qquad \text{[eq. S3]}$$

Integrating equation S1 yields equation S4, which allows the determination of ΔH_{sub}, and sublimation temperature T_{sub} from the slope and x-intercept of the plot of *ln p* vs. *1/T*, respectively:

$$\ln p = -\frac{\Delta H_{sub}}{R}\left(\frac{1}{T} - \frac{1}{T_{sub}}\right) \qquad \text{[eq. S4]}$$

Based on this approach, **Figure S2a** shows the weight loss of BiI_3 powder as a function of heating rate. The corresponding rate of weight loss (*dm/dt*) is shown in **Figure S2b**. Therefore, using equation S3, it is possible to calculate p, the vapor pressure for BiI_3. This is plotted as a semi-log plot as a function of 1/T in **Figure S2c**. As a result, the vapor pressure of BiI_3 can be calculated from equation S4. This is shown in **Figure S2d**. As stated previously, the vapor pressure of MAI is obtained from Dualeh et al. [1] Next, using the known temperature profile of the furnace, it is possible to calculate the partial vapor pressures of MAI, BiI_3 at the point of sublimation and at the point of condensation (i.e. at the substrate).

It can be seen that the MAI vapor pressure is 4.7x of vapor pressure of BiI_3 as both the precursors sublimate inside the furnace, but at different temperatures (199 ^oC for MAI and 230 ^oC for BiI_3). Since the molecules travel downstream to the cooler zone, condensation occurs. At the point of deposition, the temperature on the substrate = 160 ^oC. Here, MAI remains more volatile and the ratio of the equilibrium vapor pressure of MAI : BiI_3 = 87. Further, the driving force for condensation is proportional to $ln\ (p_{sublimation}/p_{condensation})$ which for MAI = 2.01 and for BiI_3 = 4.93. This implies that, compared to MAI, BiI_3 readily deposits on the substrate whereas,

MAI infiltrates the BiI_3 crystals via gas phase adsorption, followed by a solid-state reaction to form $MA_3Bi_2I_9$. This conclusion is in line with the observations via SEM, XRD and XPS.

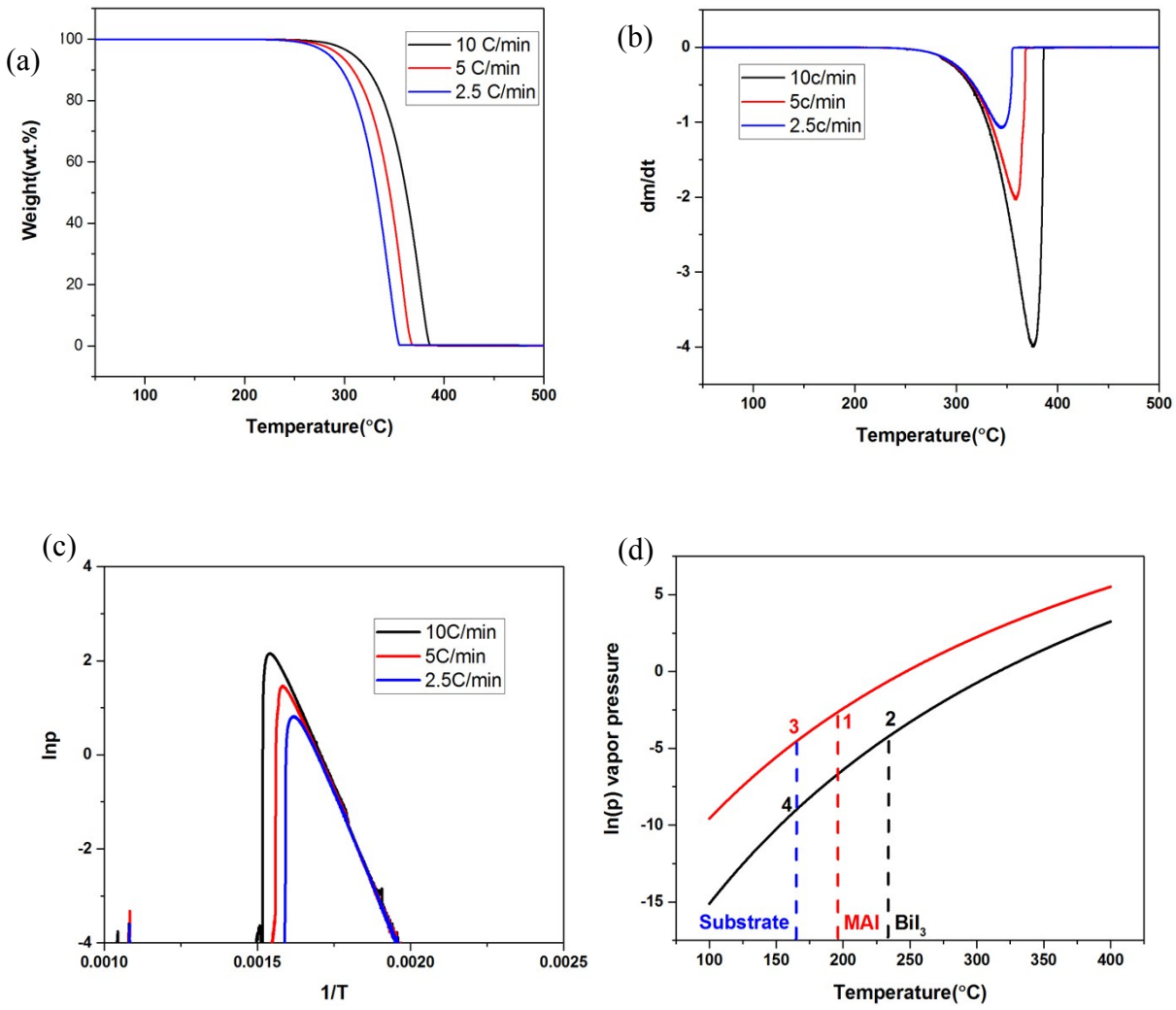

Figure S 2: (a) TGA heating curves of the BiI_3 precursor and (b) corresponding 1st derivatives measured at different heating rates of BiI_3 precursor; (c) calculated ln p vis 1/t of BiI_3 precursor. (d) vapor pressure of BiI_3 (black) and MAI (red) precursors as a function of temperature. The dotted vertical lines indicate the position where the MAI crucible (199 °C), BiI_3 crucible (230 °C) and substrate (160 °C) are placed in the horizontal tube furnace.

Precursor	ΔH_{sub} (kJ/mol)	T_{sub} (°C)
BiI_3 (this work)	128 ± 2	316 ± 2
MAI (Dualeh et al.[1])	105 ± 5	247 ± 26

Table S 1: The enthalpy of sublimation (ΔH_{sub}) and sublimation temperature (T_{sub}) are shown for both the precursors – BiI_3 and MAI. The data from BiI_3 is obtained from this work, whereas the data for MAI is obtained from the work by Dualeh et al. [1]

Supporting Information S3: Raman of BiI_3 film

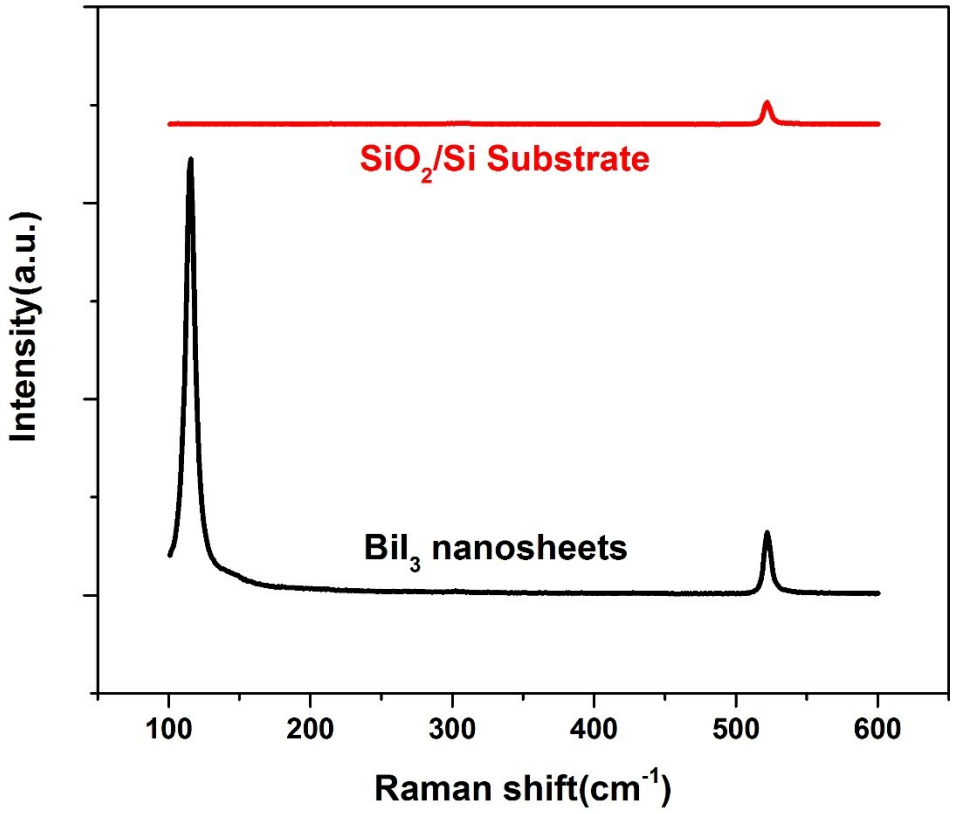

Figure S 3: Raman spectra of BiI_3 nanosheets. The Raman signal from SiO_2/Si substrate on which the BiI_3 were deposited are shown for comparison.

Supporting Information S4: XPS survey spectra of $MA_3Bi_2I_9$ film

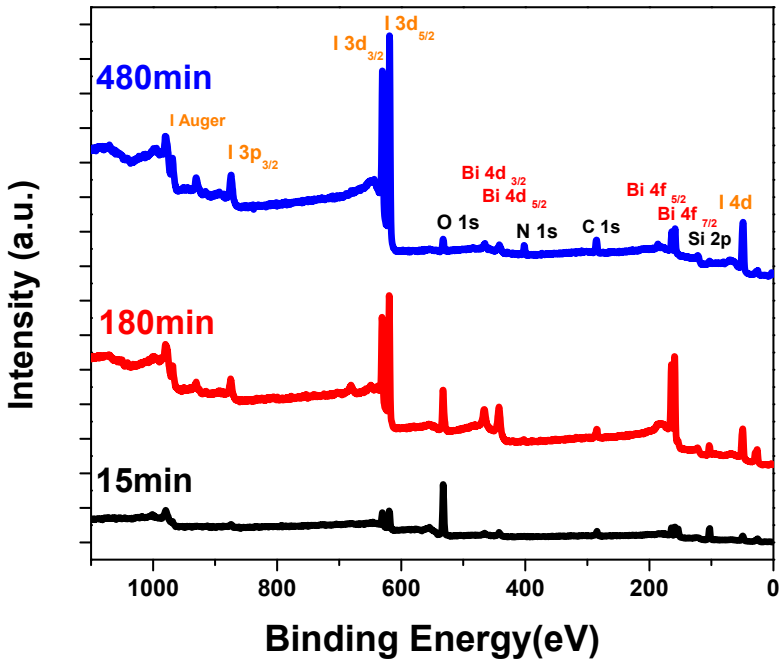

Figure S 4: XPS survey spectrum of the $MA_3Bi_2I_9$ film deposited for 15, 180 and 480 minutes, showing Bi, I, C and N peaks.

Supporting Information S5: UV-vis spectra of $MA_3Bi_2I_9$ films of various thickness

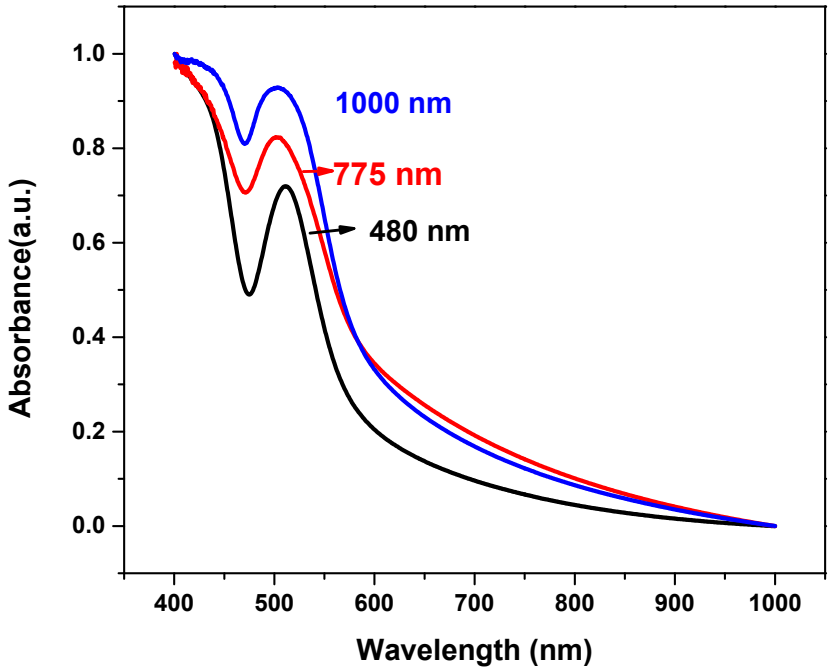

Figure S 5 : Normalized UV-vis spectra of various thickness $MA_3Bi_2I_9$ films

Supporting Information S6: Band structure using the HSE06 functional

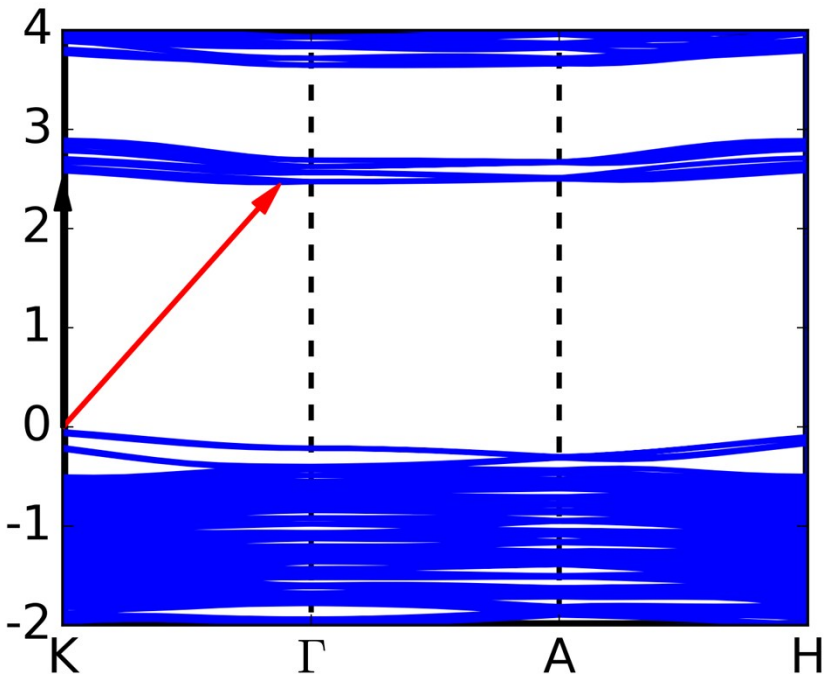

Figure S 6: Band structure for $MA_3Bi_2I_9$, using Heyd-Scucesria-Ernzerhof (HSE06) functional with spin-orbit coupling effects (SOC). The red arrow and black arrows show the indirect (2.41 eV) and direct (2.53 eV) band transitions respectively.

Supporting Information S7: SEM cross-section of $MA_3Bi_2I_9$ film

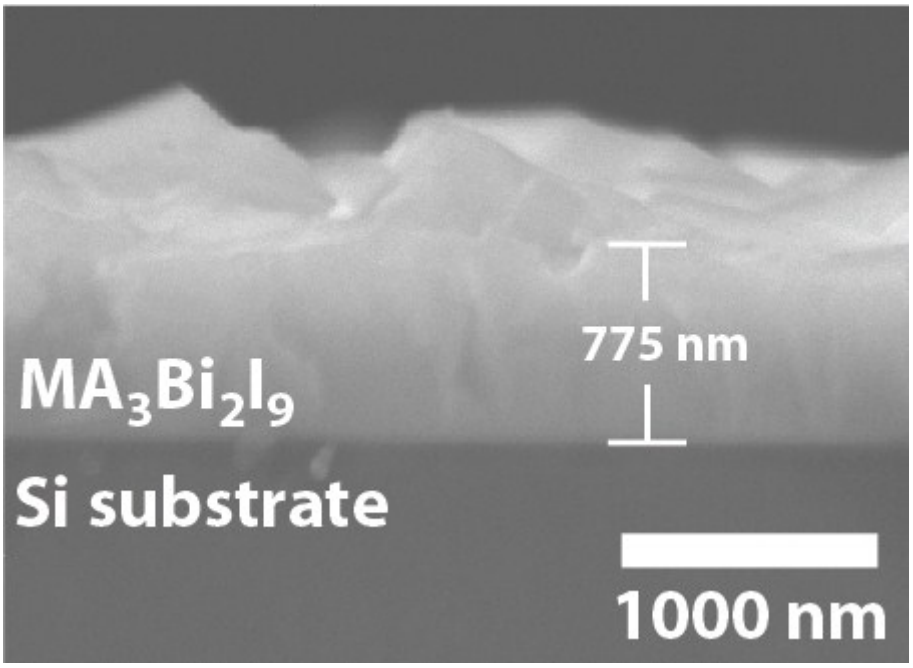

Figure S 7: Cross-section SEM image of $MA_3Bi_2I_9$ film. The thickness is determined to be 775 nm and is used in the Hall measurement calculations.

Supporting Information S7: XPS fine spectra of O 1s and Bi for fresh and 14 day exposed $MA_3Bi_2I_9$ film

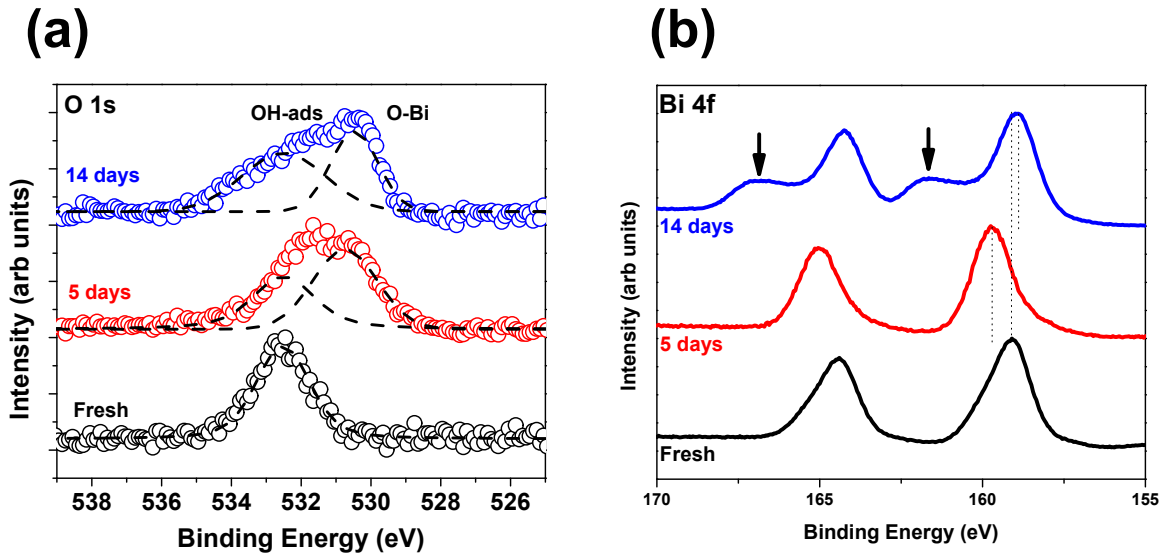

Figure S 8: (a) XPS fine spectra of O 1s for fresh (black) and after 5(red), 14 days (blue) in ambient (red). The fresh samples show O 1s peak at 532.5 eV corresponding to hydroxyl groups adsorbed on the surface of the $(MA)_3Bi_2I_9$. After 5 days, a shoulder emerges on the lower binding energy (530.4 eV) side which indicates lattice bonded oxygen with Bi which progressively grows stronger after 14 days.[4] Notice the OH peak broadens as well, signifying surface hydration. (b) XPS fine spectra of Bi 4f for fresh (black) and after 5(red) and 14 days (blue) in ambient. The Bi $4f_{7/2}$ shifts from 159 eV to 159.8 eV after 5 days. This is a result of the conversion of Bi from an iodine octahedral environment to Bi_2O_3. After 14 days the Bi $4f_{7/2}$ returns to 158.9 eV. This is because of the mixing of the oxide and iodide states of Bi to form BiOI.[5] Further, a distinct but broad shoulder appears at 161.7 eV (marked by arrows). As in the case of O 1s fine spectra, this peak is characteristic of a hydrated surface.[6]

References:

1. A. Dualeh, P. Gao, S. I. Seok, M. K. Nazeeruddin and M. Grätzel, *Chemistry of Materials*, 2014, **26**, 6160-6164.
2. M. T. Vieyra-Eusebio and A. Rojas, *Journal of Chemical & Engineering Data*, 2011, **56**, 5008-5018.
3. I. Langmuir, *Physical review*, 1913, **2**, 329.
4. X.-j. Wang, F.-t. Li, D.-y. Li, R.-h. Liu and S.-j. Liu, *Materials Science and Engineering B-Advanced Functional Solid-State Materials*, 2015, **193**, 112-120.
5. H. Liu, W. R. Cao, Y. Su, Y. Wang and X. H. Wang, *Applied Catalysis B-Environmental*, 2012, **111**, 271-279.
6. J. Chastain, R. C. King and J. Moulder, *Handbook of X-ray photoelectron spectroscopy: a reference book of standard spectra for identification and interpretation of XPS data*, Physical Electronics Division, Perkin-Elmer Corporation Eden Prairie, Minnesota, 1992.